# AE KAISER EFFECT AND ELECTROMAGNETIC EMISSION IN THE DEFORMATION OF ROCK SAMPLE

Yasuhiko Mori[1], Yoshihiko Obata[1], Jan Pavelka[2], Josef Sikula[2] and Thomas Lokajicek[3]

[1]*College of Industrial Technology, Nihon University*
*2-1, Izumi-cho 1, Narashino, Chiba 275-8575, Japan*

[2]*Czech Noise Research Laboratory, Brno University of Technology*
*Technicka 8, 616 00 Brno, Czech Republic*

[3]*Institute of Rock Structure and Mechanics*
*Academy of Sciences of the Czech Republic*
*V Holesovickach 41, 180 09 Prague 8, Czech Republic*

## ABSTRACT

Repeated loading test and simultaneous measurement of AE and electromagnetic emission were conducted on the granite samples. In the loading test, the maximum compressive load was increased step-by-step at a certain increment until the sample rupture took place to examine the Kaiser effect of the rock sample tested. The results showed that acoustic emission appeared at stress levels below the maximum previous stress, and thus the Kaiser Effect could not be clearly recognized in the rock tested. However, the electromagnetic emission appeared only when the loading stress was approached and exceeded the maximum previous stress. In the present paper, characteristics of the AE and electromagnetic emission activities are experimentally investigated and the physical meaning of the Kaiser Effect in rock sample is discussed, showing a possibility for estimating the current stress level to which rock samples have been subjected.

## 1. BACKGROUND OF AE AND EME FROM ROCK

It has been known that the changes in geoelectric potential and the anomalous radiation of geoelectromagnetic waves were observed before major earthquakes [1-4]. These phenomena also have been observed in the laboratory experiments on the rock samples, and it was found that micro- and macro-cracking processes are often accompanied by acoustic emission (AE) and electromagnetic emission (EME) [5-10].

Figure 1 shows a test result conducted on the rock sample in the laboratory [11]. In the test, the granite sample with dimensions of 75 mm x 75 mm square and height of 200 mm was deformed under the uniaxial compression stressing, and AE and EME were simultaneously measured, so that the generation of EME could be identified with the entire fracture process of the rock sample estimated by AE. Generation of AE event ($N$) starts at a level of dilatant strain of the sample ($\varepsilon$), where the dilatant strain deviates from the linear trend, and increases until the sample failure takes place. The electromagnetic emission from rock sample was detected as the

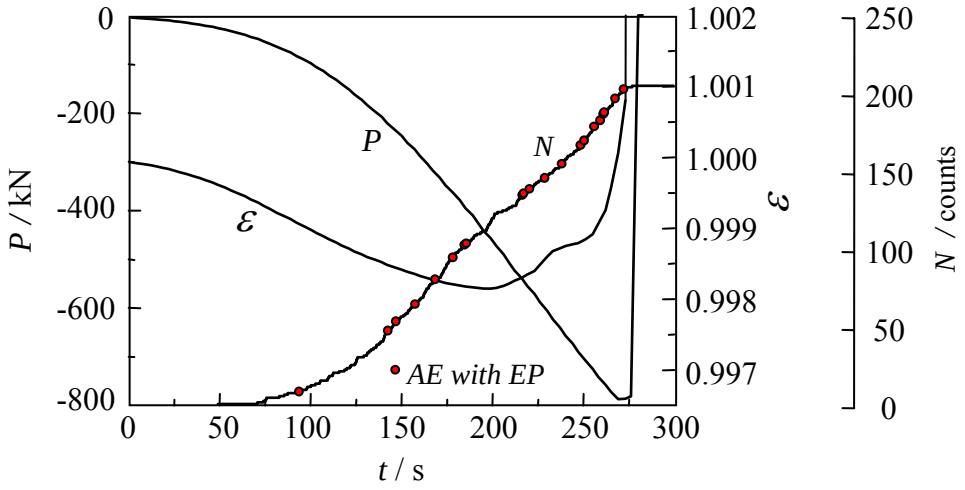


Fig. 1. AE and EME activity, load, $P$, and dilatant strain, $\varepsilon$, as a function of elapsed time, $t$, of uniaxial compression test of Inada granite sample.

electric potential (EP) change appeared between a couples of electrodes mounted on the sample surfaces. In Fig. 1, solid symbol plotted on the AE event curve denotes the AE event, which was accompanied with the EP signal. It can be said that most of the EP signals were detected at the deformation stage at which the dilatancy of the sample became significant.

In the previous studies reported, the measurements of electromagnetic emission related the rock fracture have been carried out under the monotonously increasing compressive stress in the laboratory. We also conducted the cyclic loading tests of the rock samples to characterize AE and EME generations in detail [12, 13]. In the test [13], a granite sample with dimensions of 55 mm x 35 mm square and length of 200 mm was cyclically stressed until rupture in a four-point bending frame. The function of cyclic loading was a sinusoidal

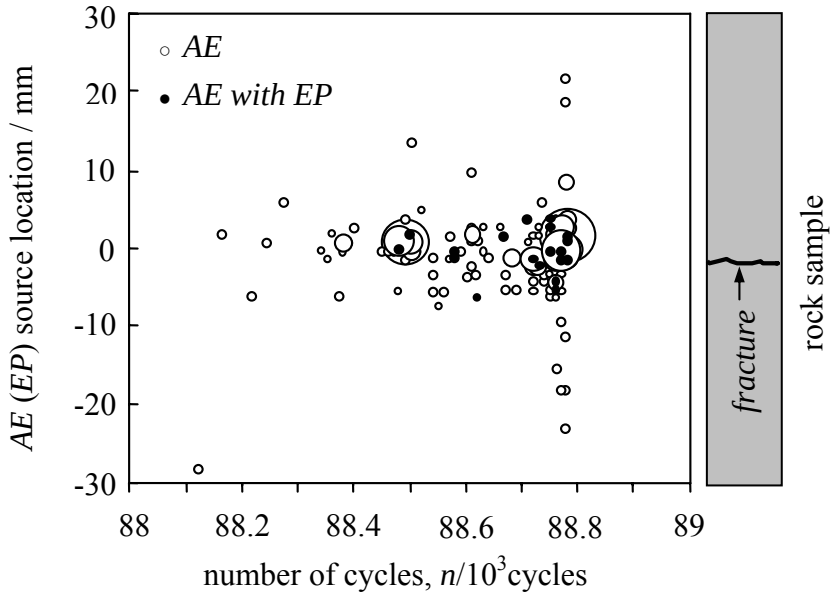


Fig. 2. Plot of AE and EME (EP) source location as a function of the number of cyclic loading. (Inada granite sample in four-point bending)

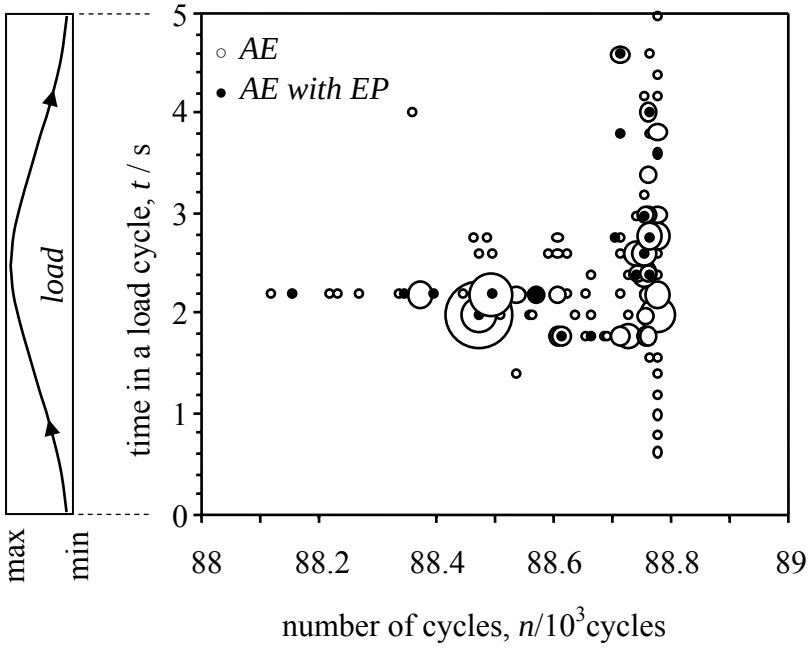


Fig. 3. Plot of AE and EME (EP) generation load level as a function of the number of cyclic loading. (Inada granite sample in four-point bending)

waveform at a frequency of 0.2 Hz with constant amplitude. Figures 2 and 3 show the important results. Figure 2 shows the AE source location plots, as a function of the number of cyclic loading. In this figure, open circles indicate the generation of AE and solid circles indicate the AE associated with the generation of EP signals, and the diameter of each circle is proportional to the event counts recorded at the point. Referring to the sketch of the fractured sample shown at the right of the figure, both the generations of AEs and the EP signals concentrate in the fractured location of the sample. On the other hand, Figure 3 shows the plot of load level at which each AE and EP event occurred, as a function of the number of cyclic loading. In the figure, y-axis is the time in a load cycle for each loading cycles, and corresponding loading waveform is shown at the left side of the plot. The meaning of the plot symbol in the figure is the same to that of Fig. 2. From this result, the AE and EP mainly occur at around the maximum load levels in a sinusoidal load. Regard to the failure of rock sample under the cyclic stressing, the authors, in our previous study, had showed the fact that new cracks appear and extend in the stage in which the stress increasing and reaches the highest level [14]. AEs also occur at fairly low load levels in the load increasing and decreasing stages just before the sample rupture. It had been found that the contact and/or the stick slip between the pre-induced fracture surfaces are the sources of those AE [14]. It must be noted that two types of acoustic emission generate in the rock sample under cyclic loading; i.e., AE due to the formation of new micro-fractures and its expansion and AE related to the frictional sliding along existing crack surfaces within a rock. Therefore, the result shown in Figs. 3 clearly demonstrates that the EP signals would be due to the nucleation of new micro crack and its extension, which were estimated by the corresponding high AE activity and the result of AE source location (Fig. 2).

The experimental results shown above obviously pointed out that the EME generates only when the fresh surfaces due to cracking are created in the material. Several theoretical models have been proposed for the explanation of EME phenomena, such as the piezo-electric

effect, the electrokinetic effect, or the electrification between the newly created surfaces [8]. The authors have proposed a model of EME generation, which is based on the movement of charged crack faces during the process of cracking [15]. On the faces of a newly created crack, the electric charges constitute an electric dipole system and due to the crack wall vibration, an EME signal is detected with a frequency corresponding to the crack length. The second source of EME signal, which is activated with a delay, is due to the whole sample mechanical vibrations with a frequency given by the sample boundary conditions. The dependence of EME and AE events on mechanical strain was investigated using a ramp increasing pressure. Events frequency is very low in the range of Hooke's law and reaches a high value near the sample breakdown. Both EME and AE signals are correlated and their amplitudes increase just before the sample rupture. This phenomenon was also observed under the cyclic deformation.

## 2. INTRODUCTION

One of the important applications of AE technique in the field of civil engineering is the determination of stress history induced in the rocks by using Kaiser effect. In the metallic materials, in general, the value of Kaiser Effect Ratio (Felicity ratio), which is defined as the ratio of the stress at which AE activity appears in the second stressing to the previously applied peak stress, ranges from 0.9 to 1.0 [16]. A ratio of 1 indicates agreement. On the other hand, in the rocks, AEs occur in the reloading process even at a stress level lower than the previously applied stress level. It can be considered that the source of such AEs are the frictional AEs, that is, the contact and/or the stick slip between the pre-induced fracture surfaces, since the micro-cracks would have been induced even at low load level in the rock during the previous loading process [14, 17].

In the Kaiser effect test on the rocks, therefore, the frictional AEs must be eliminated from the AEs measured during the second reloading process, that is, only the AEs generated from newly created cracks should be measured for evaluating the stress history in the rocks. Several methods have been proposed to distinguish the frictional AEs from the cracking AE; such as, the method of subtracting the AE activity of the second reloading from that of the first [18], the method of utilizing the *b*-value, which is defined as a slop of the AE amplitude distribution [19, 17], and the method combined the deformation rate analysis and the Kaiser effect [20, 21].

The EME signal appears only when the fractures occurred inside the material under stressing, as mentioned in the previous chapter in this paper, it is thus expected that the measuring the EME signals would directly give the recognition of the creation of fracture event. No special equipment is needed to measure the EME signals. We can make do with usual AE system by allocating one channel for the input of EME signal. The sensing device of EME signals is a coil and/or an antenna or a couple of electrodes, which are placed near or on the sample to be investigated. Such sensing device is quite simple and can be formed easily. This is also the great advantage in utilizing the EME.

In the present study, two kinds of granite sample were stressed in repeated uniaxial compression test. The sample was pre-loaded up to a certain value and then unloaded. It was then loaded to a greater value and then unloaded again. This loading-unloading procedure was repeated until the sample rupture took place. In the repeated loading test, the EME and AE signals were simultaneously measured, so that the generation of EME signals could be identified with the entire fracture process of the rock sample. EME signals were detected as the voltage changes arising across a couple of electrodes mounted on the sample surfaces. This

paper will discuss the utilization of EME for detecting the fracture event and for estimating the current stress level to which rock samples have been subjected.

## 3. EXPERIMENTAL PROCEDURE

Inada Granite and Aji Granite were chosen for the present experiment. The surface appearance of the granites is shown in Fig. 4.

Rectangular block sample with dimensions of 20 mm x 20 mm square and height of 80 mm was stressed in repeated uniaxial compression load. Schematic sample assembly is shown in Fig. 5. Both ends of the rock sample are attached to steel end pieces by epoxy resin, as shown in Fig. 5 (a), and the thickness of the epoxy fillets gradually decrease from the end pieces towards the middle of the sample, so that the stress concentration at the rock to steel contact point would be reduced. Furthermore, in order to minimize the bending in uniaxial compression due to a mismatch of loading and sample axes, a small disc of stiff paper is placed between the steel end piece and the compression apparatus, and then the load is applied to the sample. A stiff paper sheet placed between the sample end and the bottom fixed jig reduces mechanical noise and helps a good contact between them.

The sample was pre-loaded up to a certain value and then unloaded. It is then loaded to

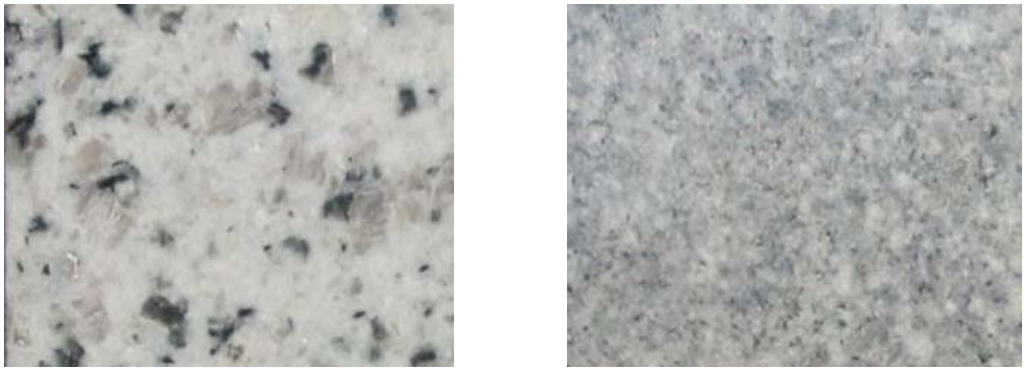

Inada Granite Aji Granite

Fig. 4. Surface appearance of granites tested.

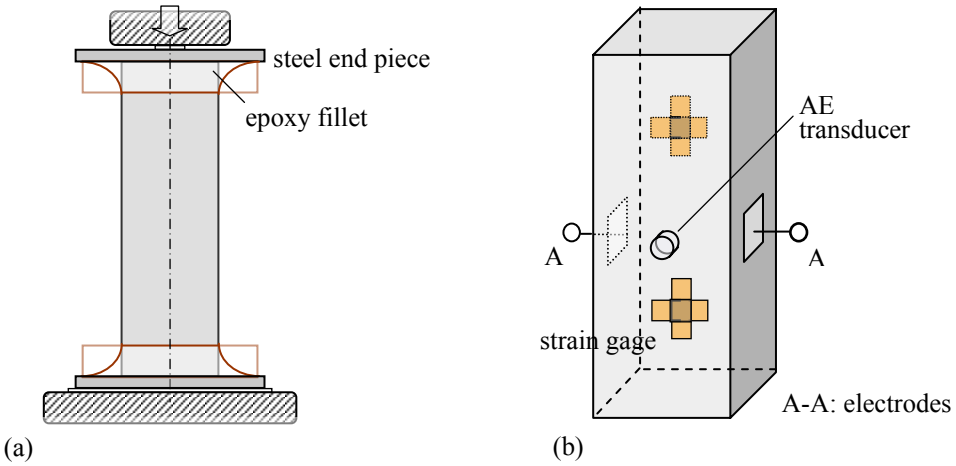


Fig. 5. Sample assembly: (a) setup for uniaxial loading and (b) arrangement of AE transducer, electrodes for EME detection, and strain gages.

a greater value and then unloaded again. This loading-unloading procedure was repeated until the sample rupture took place. Each of repeated loading-unloading procedures was conducted at a constant displacement speed of 0.5 mm/min.

AE transducer with a frequency range of 200 kHz to 700 kHz was mounted on the sample surfaces, as shown in Fig. 5 (b), to detect the AE signals during the loading test. In the present experiment, EME signal from rock sample was detected as the electric potential change appeared between two electrodes, which were formed by painting a conductive paste on the sample surfaces, as shown in Fig. 5 (b). Both the AE and electric potential (EP) signals were amplified by a 40 dB preamplifier and led into the input channels of AE system used. When an AE signal was detected at either two AE transducers the waveforms of AE and EP signals were stored on 10 bits/word memory in the AE system. AE and EP signals were digitized by 0.1 μs, and the waveforms with a time length of 0.1 x 2048 μs were stored as a single event.

Two strain gages were mounted on the sample surfaces as shown in Fig. 5 (b) (one is on the back surface) to measure the axial and horizontal strains during loading. The voltage signals from the strains and also the load cell of the loading machine were digitized and input into the separate channels of AE system.

To eliminate interference arising from ambience, the sample assembly placed on the loading frame of the test machine and the preamplifiers were shielded electromagnetically by using a heavy aluminum chamber.

## 4. RESULTS AND DISCUSSION

The results of simultaneous measurements of AE and EP signals during the repeated loading tests conducted on the Inada and Aji Granite sample are shown in Figs. 6 and 7, respectively.

The loading history for the repeated loading test is shown by the *load*, *P*, curves in the Figs. 6 and 7. After an initial load of 5 kN was applied, the maximum load level of successive loading procedures was increased in 5 kN steps until the failure of sample occurred. For the Inada Granite, the sample failure occurred at the load level of 34 kN in the procedure

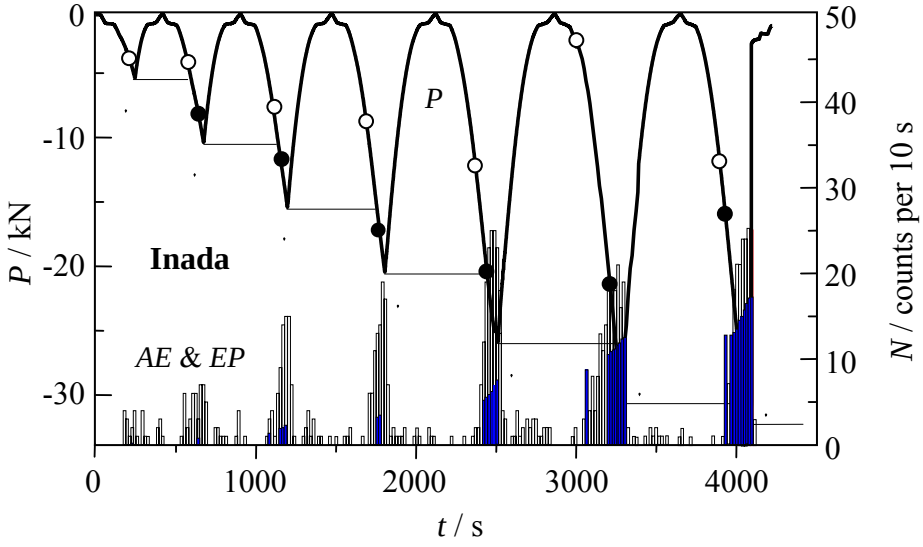


Fig. 6. History of the repeated loading test and the result of AE and EP simultaneous measurement conducted on Inada Granite sample.

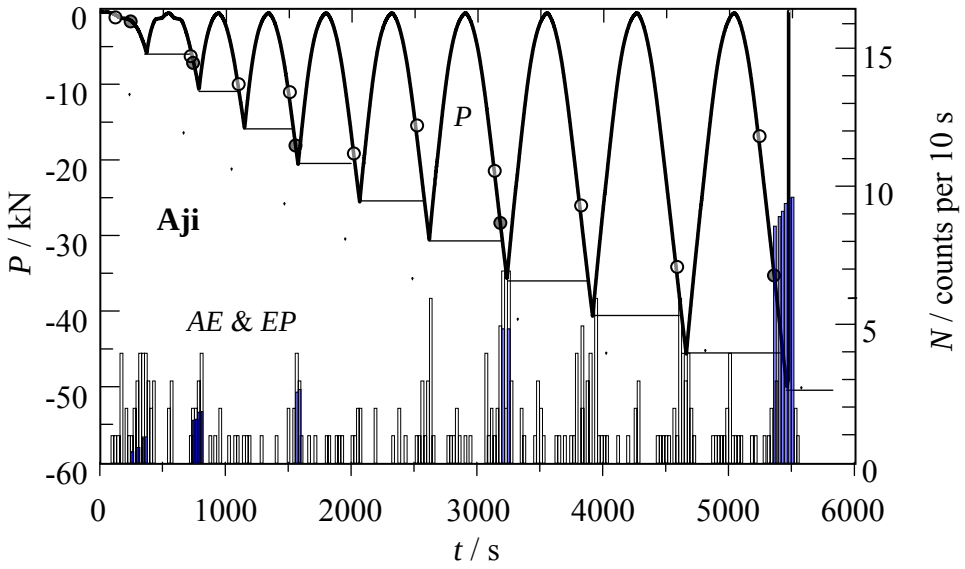


Fig. 7. History of the repeated loading test and the result of AE and EP simultaneous measurement conducted on Aji Granite sample.

#7. On the other hand, for the Aji Granite sample, the repeated loading test was finished at the maximum load level of 50 kN in the procedure #10, because of the limitation of load cell capacity used.

In the Figs. 6 and 7, the AEs measured during the repeated loading test were represented by the histogram of event count rate per 10 seconds. The black part in the AE count rate histogram denotes the AE events associated with the generation of EP signals, that is, corresponds to the rate count of EP events detected. In the present experiment, the EP signals were recognized and discriminated from the background noises by visually observing the simultaneously recorded AE and EP signal waveforms. Open symbols plotted on the load curves in the Figs. 6 and 7 denote the onset load level of active AE event generation during the road increasing stage for each repeated loading cycles. Similarly, the solid symbols on the load curves denote the onset load level of EP signals.

For the Inada Granite, Fig. 6, it is expected that the macro cracks which led the final rupture of the sample would be formed during the repeated loading procedure of #5, since the AEs generate in the unloading stage and the generation of AE starts at extremely low load level in the successive reloading procedure of #6. The AE onset load level, open symbol in Fig. 6, increases with the progress of repeated loading procedures up to the procedure #5. The load levels for each loading procedures are, however, lower than the maximum previous load applied. The values of those AE onset load levels are approximately 70 % of the maximum previous load for the #2 and #3 loadings, and are less than 60 % for the #4 and #5 loadings. Therefore, it cannot be said that the Kaiser Effect is existence in this case.

On the other hand, the occurrence of EP signals (blacked histogram in the AE count rate in the Fig. 6) begins at the loading procedure #2 and increases with the progress of the repeated loading procedures. The onset load levels of EP signals (solid symbols on the load curve) are higher values than those of AEs (open symbols) for every procedure of the loadings, and show the values almost equal to the maximum previous load, up to the procedure #5. This result clearly suggests that the emission of EP signals is associated with the creation and/or extension of micro-cracks, and is non-reversible phenomena like to what is called the Kaiser Effect of AE.

Therefore, it can be concluded that measuring the EP signals can utilize to estimate the current stress level to which the rock samples have been subjected.

The AEs, which suggest the creation of micro cracks, are observed in the initial loading #1, but no EP signals are detected until the load approaches to the level at which the EP signal firstly observed in the procedure of #2. Regard to this matter, it is considered that the micro cracks, i.e., the crack surfaces created in the early stage of loading would be small in size. The amplitude of EP signals basically depends on the amount of the electric charges re-distributed on newly created crack surfaces [15]. Such small cracks, thus, cannot emanate the EP signals, which are detectable by the AE system used.

Next, in the case of Aji Granite shown in the Fig. 7, the activity of both the AE and EP signals are low compared to those of Inada Granite shown in Fig. 6. However, the discussion done for the Inada Granite can be also concluded.

## 5. CONCLUSION

Simultaneous measurement of AE and electromagnetic emissions (EME) during the repeated uniaxial compression loading test was conducted on the Granite samples. AEs associated with the EME signal are generated only when the micro-crack is created in the sample. Measuring the EME signals could be useful for estimating the current stress level to which the rock samples have been subjected.

## ACKNOWLEDGEMENT

This research has been partially supported by JSPS Grant-in-Aid for Scientific Research in Category C of Scientific Research Grant of project No. 15560082. This research also has been partially supported by grant GACR 205/03/0071.

## REFERENCES

[1] M.B. Gokhberg, V.A. Morgunov, T. Yoshino and I. Tozawa, “Experimental measurement of electromagnetic emissions possibly related to earthquakes in Japan”, J. Geophys. Res., 87, 1982, pp.7824-7828.

[2] J.W Warwick, C. Stoker and T.R. Meyer, “Radio emission associated with rock failure: Possible application to the Great Chilean Earthquake of May 22, 1960”, J. Geophys. Res., 87, 1982, pp.2851-2859.

[3] T. Rikitake, “Nature of electromagnetic emission precursory to an earthquake”, J. Geomagnetism and Geoelectricity, Vol. 49, 1997, pp.1153-1163.

[4] N. Gershenzon, M. Gokhberg, V. Morgunov, “Sources of electromagnetic emissions preceding seismic events”, Izv Earth Phys, Vol.23, 1987, pp.127-135.

[5] U. Nitsan, “Electromagnetic emission accompanying fracture of quartz-bearing rocks” Geophys. Res. Lett., 4, 1977, pp. 333-336.

[6] T. Ogawa, K. Oike and T. Miura, “Electromagnetic radiations from rocks”, J. Geophys. Res., 90, 1985, pp.6245-6249.

[7] G. O. Cress, B. T. Brady and G. A. Rowell, “Sources of electromagnetic radiation from fracture of rock samples in the laboratory”, Geophys. Res. Lett., 14, 1987, pp. 331-334.

[8] I. Ymada, K. Masuda and H. Mizutani, “Electromagnetic and acoustic emission associated with rock fracture”, Phys. Of Earth and Planetary Interiors, 57, 1989, pp. 157-168.

[9] V. Hadjicontis and C. Mavromatou, “Transient electric signals prior to rock failure under uniaxial compression”, Geophys. Res. Lett., 21, 1994, pp. 1687-1690.
[10] T. Lolajicek and J. Sikula, “Acoustic emission and electromagnetic effects in rocks”, Progress in Acoustic Emission VIII, 1996, pp. 311-314.
[11] Y. Imaizumi, Y. Mori et al., “Measurement of acoustic and electromagnetic emission and radon emanation from rocks”, Proc. Int. Workshop on Experimental Methods in Acoustic and Electromagnetic Emission, Brno, Czech, 2002, pp. 54-62.
[12] Y. Mori, K. Sato, Y. Obata and K. Mogi, ”Acoustic emission and electric potential changes of rock samples under cyclic loading”, Progress in Acoustic Emission IX, 1998, pp. II: 1-8.
[13] I. Iida, Y. Mori, Y. Obata and K. Mogi, ”Measurement of AE and electric potential changes in fracture of brittle materials”, Progress in Acoustic Emission X, 2000, pp. 325-330.
[14] Y. Mori, K. Saruhashi and K. Mogi, “Acoustic emission from rock specimen under cyclic loading”, Progress in Acoustic Emission VII, 1994, pp. 173-178.
[15] J. Sikula, T. Lokajicek and Y. Mori, “Cracks characterisation by electromagnetic and acoustic emission”, Proceedings of 8th ECNDT, AEND, Barcelona, 2002, CDR No. 62.
[16] Y. Mori, “Kaiser Effect of acoustic emission in metals and alloys – Kaiser Effect Ratio (K. E. R.) and Microplasticity”, Proc. 4th Acoustic Emission Symposium, JSNDI, 1978, 7: 32-42.
[17] T. Shiotani, M. Ohtsu and K. Ikeda, “Detection and evaluation of AE waves due to rock deformation, Construction and Building Materials, 15, 2001, pp. 235-246.
[18] S. Yoshikawa and K. Mogi, “Experimental study on the effect of stress history on acoustic emission activity – A possibility for estimation of rock stress”, J. AE, 8, 4, 1989, pp. 113-123.
[19] T. Shiotani, K. Fujii, T. Aoki and K. Amou, “Evaluation of progressive failure using AE sources and improved b-value on slope model tests”, Progress in Acoustic Emission VII, 1994, 7: 529-534.
[20] K. Yamamoto, H. Yamamoto, N. Kato and T. Hirasawa, “Deformation rate analysis for in-situ stress estimation”, Proc. 5th Conf. On Acoustic Emission/Microseismic Activity in Geologic Structures and Materials. Trans Tech Publications, 1995, pp. 243-255.
[21] S. P. Hunt, A. G. Meyers and V. Louchnikov, “Modelling the Kaiser Effect and deformation rate analysis in sandstone using the discrete element method”, Computers and Geotechnics, 30, 2003, pp. 611-621.